Heat transfer modelling in the Si–Ge nanoparticle composites by numerical solution of the equation of phonon radiative transfer

Meysam Mohamadi[1] ✉, *Mozaffar A. Mehrabian*[1], *Afrasiab Raisi*[2]

[1]*Department of Mechanical Engineering, Shahid Bahonar University of Kerman, Kerman, Iran*
[2]*Department of Mechanical Engineering, Shahrekord University, Shahrekord, Iran*
✉ *E-mail: mohamadi.meysam@eng.uk.ac.ir*

Published in Micro & Nano Letters; Received on 13th February 2018; Accepted on 20th February 2018

Phonon Boltzmann transport equation and consequently the Equation of Phonon Radiative Transfer govern the conductive heat transfer in semiconductors at the nanoscale. Here a semiconducting nanoparticle composite, consisting of cubic *Si* nanoparticles in a *Ge* substrate is considered. A detailed three-dimensional heat transfer analysis is done, the temperature distributions are generated, the Effective Thermal Conductivity (ETC) of the nanocomposite is obtained, and the effect of the *Si* nanoparticle size and the constituents' atomic percentage on the ETC is explored. As the most comprehensive study, the effect of the interface density on the ETC is investigated and the results are compared with those obtained using the Monte Carlo simulation. The results show that at a fixed atomic percentage, as the dimensions are decreased, the ETC reduces and the temperature jumps become larger. At a fixed Si nanoparticle size, as the Ge atomic percentage increases, the ETC also increases, and the ETC reduces as the interface density increases. Reducing the ETC is a way to improve the thermoelectric energy conversion.

1. Introduction: The solid state nanoscale heat transfer can be modelled at three different levels of descriptions that are microscopic, mesoscopic and macroscopic [1]. Microscopic methods provide atomic scale information like the first-principle method and the molecular dynamics (MD) simulation. Mesoscopic methods produce statistical information such as the particle distribution function and are mostly derived from Boltzmann transport equation such as the equation of phonon radiative transfer (EPRT), Monte Carlo (MC) simulation, and the lattice Boltzmann method (LBM). Finally, the macroscopic methods use only several state variables for continuum media such as phonon hydrodynamic model [2], dual-phase-lag model, ballistic–diffusive model, and thermon gas model.

According to the case, one or more than one [3–5] of the aforementioned methods have been used to study the thermal properties of the semiconductor structures, namely the best thermoelectric materials. The efficiency of the thermoelectric devices is determined by the dimensionless figure-of-merit as follows:

$$ZT = S^2 \sigma T / k \tag{1}$$

where S is the Seebeck coefficient, s is the electrical conductivity, and k is the thermal conductivity [6, 7]. According to (1), the thermal conductivity reduction enhances the figure-of-merit. Whereas the phonons have the major role in thermal conductivity of semiconductor structures, phonon transport, and its scattering have been investigated in the past [8–13]. Raisi and Rostami [14] investigated the unsteady heat transport in a *GaAs/AlAs* superlattice in the direction perpendicular to the layers by means of the EPRT. Yang and Chen [15] modelled the Effective Thermal Conductivity (ETC) of a SiGe nanocomposite consisting of squared silicon nanowires in a germanium host. They solved the EPRT and obtained the thermal conductivity of the nanocomposite in the direction of heat transfer, which is perpendicular to the nanowires. Lukes and Tien [16] used MD simulation to achieve thermal conductivity in a thin nanoporous layer. Yang *et al.* [17] obtained the thermal conductivity of a nanocomposite consisting of circular silicon nanowires in a germanium host longitudinally. Minnich *et al.* [18] used the Boltzmann transport equation considering the relaxation-time approximation to calculate the thermoelectric properties of n-type and p-type SiGe nanocomposites. Zhou *et al.* [19] presented a semiclassical model for thermoelectric transport in nanocomposites. They developed a semiclassical electron transport model based on the Boltzmann transport equation to describe the thermoelectric transport processes in semiconductor nanocomposites. Also, the LBM has been employed to study the phonon transport in various nanostructures [20, 21]. Garg and Chen [22] employed the density functional perturbation theory to compute the thermal conductivity of a SiGe superlattice. Hua and Cao [23] employed the phonon Boltzmann transport equation to derive a model for the ETC of multiple-constrained silicon-based nanostructures. Zhou *et al.* [24] investigated the thermoelectric transport properties of n-type silicon-based superlattice-nanocrystalline heterostructures by first-principles and MD simulations combined with the Boltzmann transport theory. Their results show that nanostructuring the superlattice structure can further reduce the thermal conductivity while the electrical transport properties remain approximately at the bulk level, and provides a new way for enhancing the thermoelectric performance of the silicon-based nanostructures.

In this research, for the first time, we study the three-dimensional (3D) conductive heat transfer in a nanocomposite consisted of *Si* nanoparticles in a *Ge* substrate by solving the EPRT numerically. The influence of the size of *Si* nanoparticles and the atomic percentage of the constituents on the temperature distributions and on the ETC will be explored. Finally, the ETC of the nanoparticle composite is obtained as a function of the interface density and the results are compared with the MC simulation.

2. Research perspective: A nanocomposite consisting of cubic *Si* nanoparticles located in the *Ge* substrate regularly is shown in Fig. 1. It is assumed that the heat is forced to flow only in one direction, namely x. To study this nanocomposite, we can select a periodic unit cell consisting of the *Si* cubic particle located in the centre of a cubic Ge particle as shown in Fig. 2.

3. Governing equations: Conductive heat is transferred in solids by means of electrons and phonons. In the semiconductors the most effective carriers of the thermal energy are phonons. In conventional conductive heat transfer where the spatial and time

doi: 10.1049/mnl.2018.0128

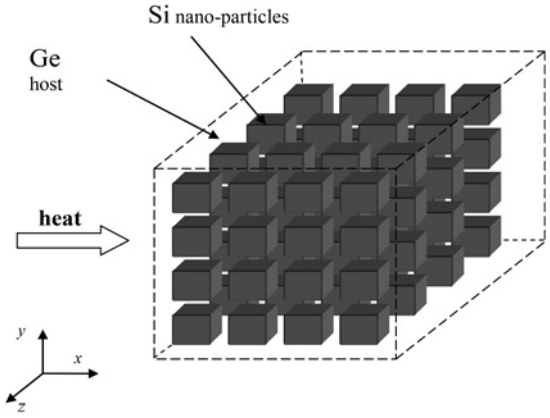

Fig. 1 *Si–Ge nanoparticle composite and the heat flow direction, in the Cartesian coordinates*

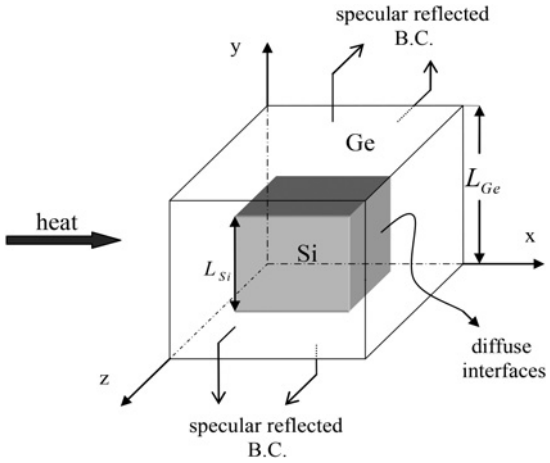

Fig. 2 *Periodic unit cell of the nanocomposite, considered as the domain of the heat transfer study*

dimensions and scales are macroscopic, the Fourier's law of thermal conduction is valid and the thermal conductivity relation, based on the kinetic theory is as follows:

$$k = \left(\frac{1}{3}\right) C v \Lambda \tag{2}$$

where C is the volumetric specific heat, v isthe phonon group velocity, and Λ is the phonon mean free path (MFP). If the characteristic length is nearly equal or smaller than Λ, due to the ballistic nature of phonons, (2) is not valid, and also the Fourier's law is not applicable.

In this research, we assume that the wave features of the phonons are negligible and they behave as particles. Thus the phonon Boltzmann equation (PBE) is used as the fundamental governing equation. Using single relaxation time assumption, and without any external force, PBE is expressed as follows:

$$\frac{\partial f}{\partial t} + v \cdot \nabla f = \frac{f^0 - f}{\tau_r} \tag{3}$$

where f is the phonons' distribution function, v is the phonons' group velocity, τ_r is the relaxation time, and the superscript 0 shows the equilibrium state. The 'total phonon intensity' defined as follows can be substituted for phonons' distribution function:

$$I_i = \frac{1}{4\pi} \sum_m \int_0^{\omega_{\max}} |v_{mi}| \hbar \omega D_{mi}(\omega) d\omega \tag{4}$$

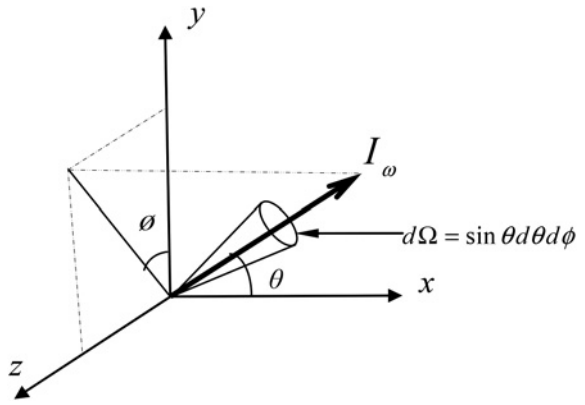

Fig. 3 *Coordinate system, the polar, and azimuthal angles*

In this relation, the subscript i indicates the material ($i = 1$ refers to germanium and $i = 2$ refers to silicon), $D(\omega)$ is the density of states per unit volume, f is the phonons' distribution function, $\hbar$ is the Plank's constant, $|v_{mi}|$ is the phonons' group velocity magnitude, ω is the phonons' frequency, $\omega_{\max}$ is the phonons' maximum frequency for each polarisation, and the subscript m shows three polarisations of phonons. In steady-state conditions, using the total phonon intensity, EPRT is obtained from (3) and can be written as follows:

$$\begin{aligned} &v_x \frac{\partial I}{\partial x} + v_y \frac{\partial I}{\partial y} + v_z \frac{\partial I}{\partial z} = \frac{I_0 - I}{\tau_r} \\ &v_x = v\cos\theta, \quad v_y = v\sin\theta\cos\phi, \quad v_z = v\sin\theta\sin\phi \end{aligned} \tag{5}$$

After substitution and simple manipulations, the EPRT can be written as

$$\cos\theta_i \frac{\partial I_i}{\partial x} + \sin\theta_i \cos\phi_i \frac{\partial I_i}{\partial y} + \sin\theta_i \sin\phi_i \frac{\partial I_i}{\partial z} = \frac{I_{0i} - I_i}{\Lambda_i} \tag{6}$$

where $\Lambda_i$is the average phonons' mean free path of each material, the product of relaxation time and group velocity magnitudes, and I_{0i} is the equilibrium phonon intensity defined as

$$\begin{aligned} I_{0i}(x, y, z) &= \frac{1}{4\pi} \int_{4\pi} I_i(r, \Omega)\, \mathrm{d}\Omega \\ &= \frac{1}{4\pi} \int_0^{2\pi} \int_0^{\pi} I_i(x, y, z, \theta, \phi) \sin\theta\, \mathrm{d}\theta\, \mathrm{d}\phi \end{aligned} \tag{7}$$

where Ωdenotes the solid angle, θ is the polar, and ϕ is the azimuthal angle as shown in Fig. 3.

4. Interfaces and the boundaries: As stated before according to Fig. 2 for determining the phonons intensities in all directions in the domain of Si and Ge, we can use (6) and (7). For interfaces and boundaries, we should note that according to the mathematical structure of the Boltzmann transport equation, the intensities entering the domain, should be specified from boundary and interface conditions. For example, according to Figs. 2 and 4, in the left boundary ($x = 0$), intensities in the negative x-direction, can be achieved from (6) and (7) but those in the positive x-direction, should be specified as boundary conditions. Therefore, boundaries ($x = 0$) and ($x = L_{\mathrm{Ge}}$) are subject to the periodic boundary condition as follows:

$$I(L_{\mathrm{Ge}}, y, z, \theta, \phi) - I_0(L_{\mathrm{Ge}}, y, z) = I(0, y, z, \theta, \phi) - I_0(0, y, z) \tag{8}$$

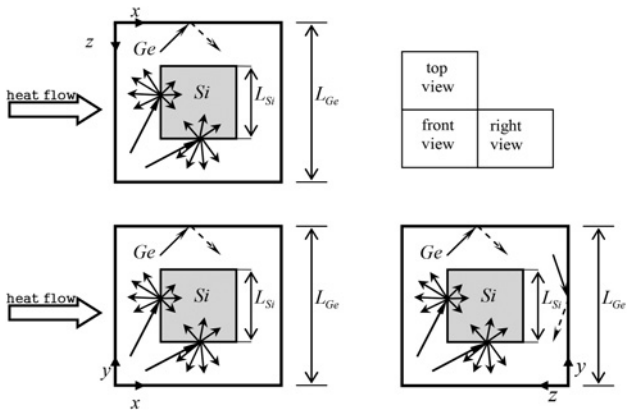

Fig. 4 *Boundary and interface conditions for unit cell*

While heat only flows in the x-direction, on the boundaries $(y=0)$, $(y=L_{\mathrm{Ge}})$, $(z=0)$, and $(z=L_{\mathrm{Ge}})$ the specular reflection boundary condition is implemented as follows:

$$\begin{aligned} I(x, L_{\mathrm{Ge}}, z, \theta, \phi) &= I(x, L_{\mathrm{Ge}}, z, \theta, \pi-\phi) \\ I(x, 0, z, \theta, \phi) &= I(x, 0, z, \theta, \pi-\phi) \\ I(x, y, L_{\mathrm{Ge}}, \theta, \phi) &= I(x, y, L_{\mathrm{Ge}}, \theta, -\phi) \\ I(x, y, 0, \theta, \phi) &= I(x, y, 0, \theta, -\phi) \end{aligned} \tag{9}$$

The scattering of the phonons at the interfaces is diffuse and the transmissivity and reflectivity of the interfaces are obtained from the diffuse mismatch model and calculated as follows:

$$T_{21}=R_{12}, \quad R_{12}+T_{12}=1, \quad T_{12}=C_2v_2/(C_1v_1+C_2v_2) \tag{10}$$

where T denotes the transmissivity, R is the reflectivity and the subscript 12 means from medium one to medium two. As an example in the left interface ($x_1 = L_{\mathrm{Ge}}/2 - L_{\mathrm{Si}}/2$) and in the positive x-direction, the total phonon intensity that has a constant value in the right hemisphere is achieved from the conservation of energy as follows:

$$\begin{aligned} I(x_1, y, z, \theta, \phi) = &-\frac{R_{21}}{\pi}\int_0^{2\pi}\int_{\pi/2}^{\pi} I_2(x_1, y, z, \theta, \phi)\cos\theta\sin\theta\,\mathrm{d}\theta\,\mathrm{d}\phi \\ &+\frac{T_{12}}{\pi}\int_0^{2\pi}\int_0^{\pi/2} I_1(x_1, y, z, \theta, \phi)\cos\theta\sin\theta\,\mathrm{d}\theta\,\mathrm{d}\phi \end{aligned} \tag{11}$$

5. Temperature field and thermal conductivity modelling: Although at the nanoscale the temperature is not a criterion of local thermal equilibrium, the temperature can be defined as the local energy density as follows [15]:

$$T(x, y, z) = \frac{4\pi I_0(x, y, z)}{C|v|} \tag{12}$$

The average temperature in each surface perpendicular to the heat transfer flow can be achieved as follows:

$$\bar{T}(x) = \frac{1}{L_{\mathrm{Ge}}^2}\int_0^{L_{\mathrm{Ge}}}\int_0^{L_{\mathrm{Ge}}} T(x, y, z)\,\mathrm{d}y\,\mathrm{d}z \tag{13}$$

The x-component heat flux and the rate of heat transfer can be obtained from the total phonon intensity as follows:

$$\begin{aligned} q_x(x, y, z) &= \int_0^{2\pi}\int_0^{\pi} I(x, y, z, \theta, \phi)\cos\theta(\sin\theta\,\mathrm{d}\theta\,\mathrm{d}\phi) \\ Q_x(x) &= \int_0^{L_{\mathrm{Ge}}}\int_0^{L_{\mathrm{Ge}}} q_x(x, y, z)\,\mathrm{d}y\,\mathrm{d}z \end{aligned} \tag{14}$$

Indeed, because of the specular boundary conditions in y and z directions, the rate of heat transfer is independent of x and is constant. The ETC can be modelled with a similar formulation of the Fourier's law for heat transfer across a single layer thin wall, as follows:

$$\begin{aligned} Q_x &= k_{\mathrm{eff}}(L_{\mathrm{Ge}}^2)\frac{\left(\bar{T}(0)-\bar{T}(L_{\mathrm{Ge}})\right)}{L_{\mathrm{Ge}}}, \\ k_{\mathrm{eff}} &= \frac{Q_x}{L_{\mathrm{Ge}}\left(\bar{T}(0)-\bar{T}(L_{\mathrm{Ge}})\right)} \end{aligned} \tag{15}$$

The method implemented for the numerical solution of the EPRT [25] is based on the finite difference method and is similar to the discrete ordinate method in thermal radiation. A detailed computer programming is applied to extract the results in 25 different cases. Some parameters used for the calculation are presented in Table 1 [15].

6. Results and discussion: In presenting the results, we use x^*, y^*, and z^*, instead of x, y, and z, whereas $x^*=x/L_{\mathrm{Ge}}$, $y^*=y/L_{\mathrm{Ge}}$, and $z^*=z/L_{\mathrm{Ge}}$. x_1^*, y_1^*, and z_1^* indicate the first interfaces in the x, y, and z directions, respectively, while x_2^*, y_2^*, and z_2^* represent the second interfaces. Another parameter is the atomic percentage of the constituents in the nanocomposite representing the ratio of L_{Ge} to L_{Si}.

In Figs. 5–10, the *Ge* atomic percentage is selected 78%, which corresponds to $L_{\mathrm{Ge}}/L_{\mathrm{Si}}$ being 1.714. According to the phonon MFP of Si at room temperature, three different values of Si lengths are

Table 1 Room-temperature parameters used in the calculations

	C, J/m^{3}K	v, m/s	k, W/mK	Λ, nm
Si	930,000	1804	150	268
Ge	870,000	1042	60	198

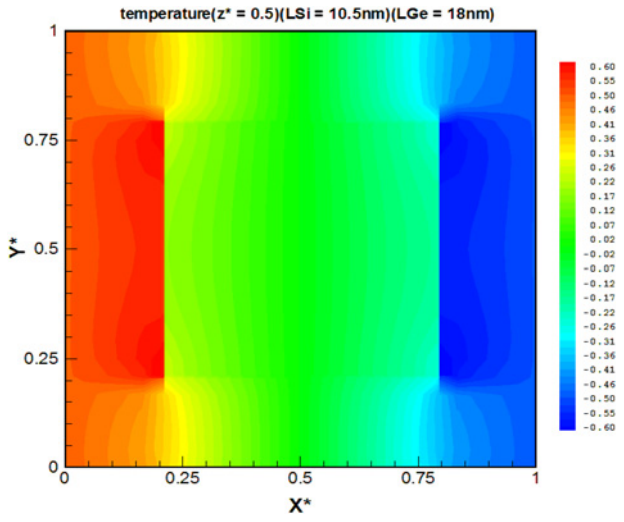

Fig. 5 *Temperature contours $z^*=0.5$, $L_{Si}=10.5$ nm, $L_{Ge}=18$ nm*

doi: 10.1049/mnl.2018.0128

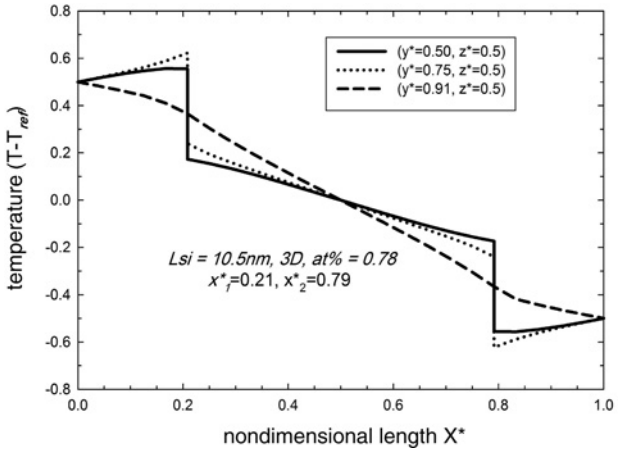

Fig. 6 *Temperature profiles $z^* = 0.5$, $L_{Si} = 10.5$ nm, $L_{Ge} = 18$ nm, $y^* = 0.5$, $y^* = 0.75$, $y^* = 0.91$*

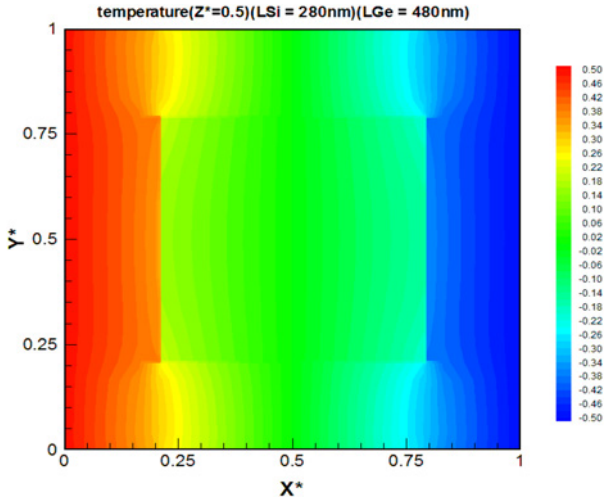

Fig. 7 *Temperature contours $z^* = 0.5$, $L_{Si} = 280$ nm, $L_{Ge} = 480$ nm*

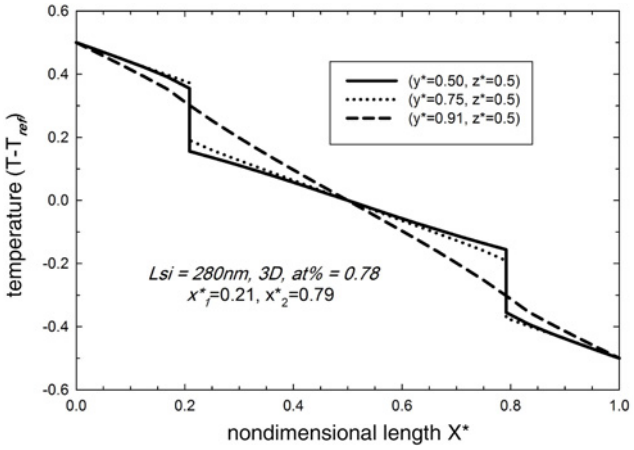

Fig. 8 *Temperature profiles $z^* = 0.5$, $L_{Si} = 280$ nm, $L_{Ge} = 480$ nm, $y^* = 0.5$, $y^* = 0.75$, $y^* = 0.91$*

selected as 10.5, 280, and 831 nm to present a more comprehensive analysis. The temperature contours in the surface $z^* = 0.5$ are plotted in Figs. 5, 7 and 9 and also the temperature profiles for three different values of y^*, in the surface $z^* = 0.5$ are shown in Figs. 6, 8 and 10. In Figs. 5 and 6 ($L_{Si} = 10.5$ nm), since the Si nanoparticle size is much smaller than the phonon MFP, the ballistic

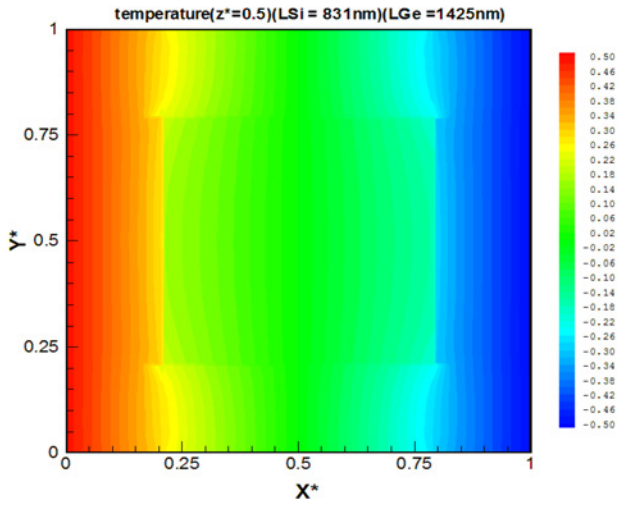

Fig. 9 *Temperature contours $z^* = 0.5$, $L_{Si} = 831$ nm, $L_{Ge} = 1425$ nm*

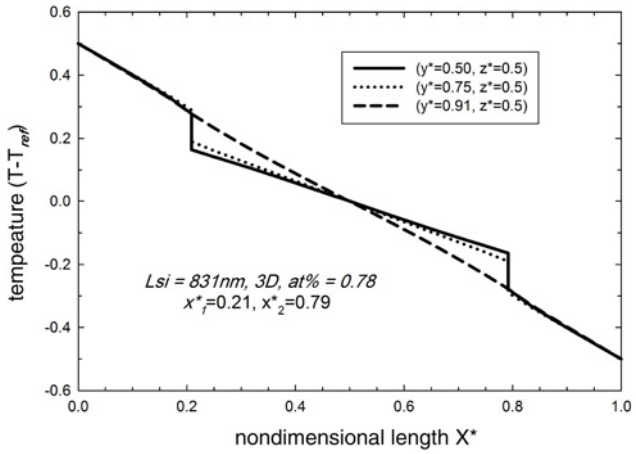

Fig. 10 *Temperature profiles $z^* = 0.5$, $L_{Si} = 831$ nm, $L_{Ge} = 1425$ nm, $y^* = 0.5$, $y^* = 0.75$, $y^* = 0.91$*

effects of phonon heat transfer is completely dominant and large temperature jumps are seen at the interfaces perpendicular to the heat flow. Here the temperature jump in the centreline ($z^* = 0.5$ and $y^* = 0.5$) is 0.3818 K. In such cases, high thermal resistance at perpendicular interfaces causes this temperature jump, and increases the total thermal resistance of the nanoparticle composite and consequently reduces the ETC. In this case, the ETC is 5.268 W/mK. As shown in Fig. 5, despite the important role of the perpendicular interfaces, the parallel interfaces do not have notable effects on thermal resistance as they have a little influence on the temperature field. A notable behaviour shown in Fig. 6 is that the temperature gradient in some regions is positive that does not happen in macroscales when the temperature gradient should be negative in the heat flow direction as shown in Fig. 10 and even Fig. 8. It seems to have a contradiction with the second law of thermodynamics. As mentioned before, at the nanoscale the temperature is not defined as the thermal equilibrium case, but it is defined as the local energy density according to (12). In the case of Figs. 5 and 6, the ballistic transport is dominant and no local thermal equilibrium can be established and the calculated temperature represents the local energy density. A detailed illustration is available in [15] for a similar case based on the thermal radiation analysis in the phonon ballistic range. In Figs. 7 and 8 ($L_{Si} = 280$ nm), both ballistic and diffusive effects are present. The temperature jump in the centreline is 0.1993 K and the ETC is 42.43 W/mK. In Figs. 9 and 10 ($L_{Si} = 831$ nm), the diffusive

regime is dominant and the ballistic effects start to vanish. The temperature jump in the centreline is only 0.1142 K and the ETC is 55.67 W/mK. Between the parallel interfaces in Figs. 5, 7 and 9, the shape of the temperature contours are approximately similar and indicate that the parallel interfaces have a little contribution to the ETC reduction. In Fig. 11, the average temperature profiles for the three preceding cases are shown. As stated before the temperature jump decreases as the Si nanoparticle size increases. It is interesting to mention that in all sections of these profiles even for the case ($L_{Si} = 10.5$ nm), in spite of Fig. 6, the temperature profiles are always descending.

In Fig. 12, the change of ETC versus *Ge* atomic percentage is shown for two *Si* nanoparticle sizes of 10 and 50 nm. In this figure, the 3D deterministic method based on EPRT is compared with the MC simulation [26]. As shown in Fig. 12, at a fixed *Si* nanoparticle size, as the Ge atomic percentage increases, the ETC also increases. The diagrams show that the two methods have the same behaviour but the ETC in our work is slightly less than the MC.

At a fixed atomic percentage of the constituents, as the size of *Si* particles increase, the ETC also increases and approaches to the bulk values. An example for 78% of the *Ge* atomic percentage is shown in Fig. 13.

The most comprehensive parameter is the interface density that covers the atomic percentage and also the size of the nanoparticles, which can be calculated from these two parameters. In Fig. 14, the ETC of the nanoparticle composite plots versus the interface

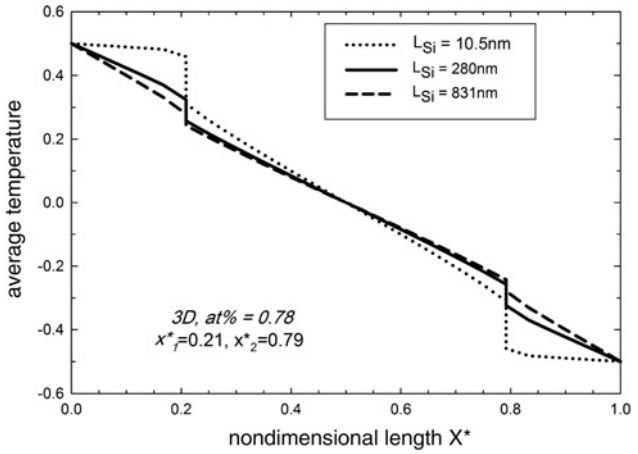

Fig. 11 *Average temperature profiles $L_{Si} = 10.5$, 280, 831 nm*

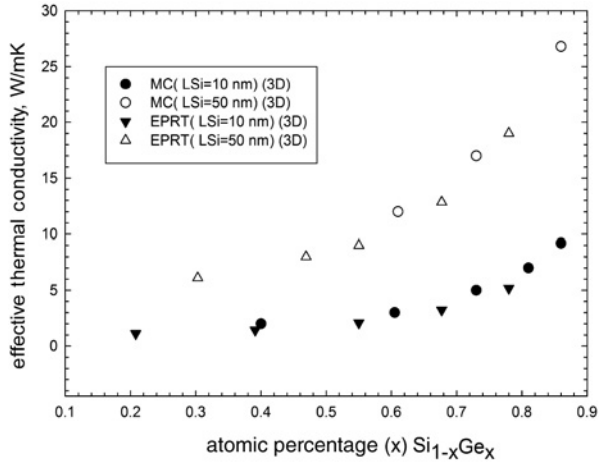

Fig. 12 *ETC versus the Ge atomic percentage, comparison of MC simulation [26] and our 3D solution based on EPRT*

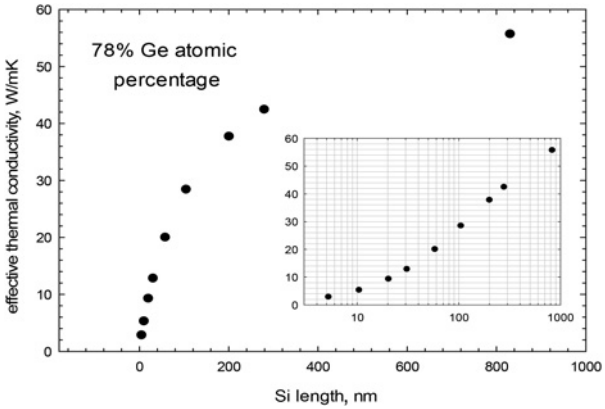

Fig. 13 *ETC versus Si nanoparticle size with 78% Ge atomic percentage*

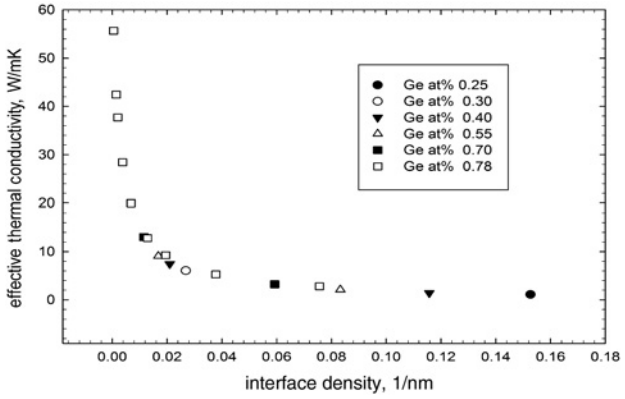

Fig. 14 *ETC versus interface area per unit volume (interface density)*

density. By increasing the summation of perpendicular interfaces of nanoparticles per each cubic nanometre, the ETC is reducing. A check point is that by approaching the interface density to zero, the ETC approaches the bulk *Ge* thermal conductivity (60 W/mK).

7. Concluding remarks: In this research, an extensive 3D study on the conductive heat transfer in the *Si–Ge* nanoparticle composites has been done. The EPRT has been solved numerically and some of the results are as follows:

Thermal conductivity in nanostructures does not only depend on the material of the constituents but also depends on dimensions and sizes.

At fixed atomic percentage, as the dimensions are decreased, the ETC reduces and the temperature jumps become larger. At fixed *Si* nanoparticle size, as the *Ge* atomic percentage increases, the ETC also increases, and the ETC reduces as the interface density increases.

The ETC values obtained, are approximately the same as the MC simulation results and the deviation is ∼10%.

By employing semiconductor nanocomposites, the thermal conductivity reduces, and consequently, the figure-of-merit becomes larger and the efficiency of thermoelectric devices improves.

8 References

[1] Guo Y., Wang M.: 'Phonon hydrodynamics and its applications in nanoscale heat transport', *Phys. Rep.*, 2015, **595**, pp. 1–44

[2] Sellitto A.: 'A phonon-hydrodynamic approach to thermal conductivity of Si–Ge quantum dot superlattices', *Appl. Math. Model.*, 2015, **39**, (16), pp. 4687–4698

doi: 10.1049/mnl.2018.0128

[3] Li L., Zhou L., Yang M.: 'An expanded lattice Boltzmann method for dual phase lag model', *Int. J. Heat Mass Transf.*, 2016, **93**, pp. 834–838
[4] Zhou Y., Zhang X., Hu M.: 'Nonmonotonic diameter dependence of thermal conductivity of extremely thin Si nanowires: competition between hydrodynamic phonon flow and boundary scattering', *Nano Lett.*, 2017, **17**, (2), pp. 1269–1276
[5] Zhou Y., Gong X., Xu B., *ET AL.*: 'Decouple electronic and phononic transport in nanotwinned structures: a new strategy for enhancing the figure-of-merit of thermoelectrics', *Nanoscale*, 2017, **9**, (28), pp. 9987–9996
[6] Nolas G.S., Sharp J., Goldsmid J.: 'Thermoelectrics: basic principles and new materials developments' (Springer Science & Business Media, Berlin, 2013)
[7] Kajikawa T., Rowe D., Rowe D.: 'Thermoelectric handbook: macro to nano', (CRC/Taylor & Francis, Boca Raton, FL, USA, 2006)
[8] Casimir H.: 'Note on the conduction of heat in crystals', *Physica*, 1938, **5**, (6), pp. 495–500
[9] Holland M.: 'Phonon scattering in semiconductors from thermal conductivity studies', *Phys. Rev.*, 1964, **134**, (2A), p. A471
[10] Pohl R., Stritzker B.: 'Phonon scattering at crystal surfaces', *Phys. Rev. B*, 1982, **25**, (6), p. 3608
[11] Klitsner T., VanCleve J., Fischer H.E., *ET AL.*: 'Phonon radiative heat transfer and surface scattering', *Phys. Rev. B*, 1988, **38**, (11), p. 7576
[12] Joshi A., Majumdar A.: 'Transient ballistic and diffusive phonon heat transport in thin films', *J. Appl. Phys.*, 1993, **74**, (1), pp. 31–39
[13] Ioffe A.F.: 'Semiconductor thermoelements and thermoelectric cooling' (Infosearch Limited, London, 1957)
[14] Raisi A., Rostami A.A.: 'Unsteady heat transport in direction perpendicular to a double-layer thin-film structure', *Numer. Heat Transf. A, Appl.*, 2002, **41**, (4), pp. 373–390
[15] Yang R., Chen G.: 'Thermal conductivity modeling of periodic two-dimensional nanocomposites', *Phys. Rev. B*, 2004, **69**, (19), p. 195316
[16] Lukes J.R., Tien C.: 'Molecular dynamics simulation of thermal conduction in nanoporous thin films', *Microscale Thermophys. Eng.*, 2004, **8**, (4), pp. 341–359
[17] Yang R., Chen G., Dresselhaus M.S.: 'Thermal conductivity of simple and tubular nanowire composites in the longitudinal direction', *Phys. Rev. B*, 2005, **72**, (12), p. 125418
[18] Minnich A., Lee H., Wang X., *ET AL.*: 'Modeling study of thermoelectric SiGe nanocomposites', *Phys. Rev. B*, 2009, **80**, (15), p. 155327
[19] Zhou J., Li X., Chen G., *ET AL.*: 'Semiclassical model for thermoelectric transport in nanocomposites', *Phys. Rev. B*, 2010, **82**, (11), p. 115308
[20] Nabovati A., Sellan D.P., Amon C.H.: 'On the lattice Boltzmann method for phonon transport', *J. Comput. Phys.*, 2011, **230**, (15), pp. 5864–5876
[21] Guo Y., Wang M.: 'Lattice Boltzmann modeling of phonon transport', *J. Comput. Phys.*, 2016, **315**, pp. 1–15
[22] Garg J., Chen G.: 'Minimum thermal conductivity in superlattices: a first-principles formalism', *Phys. Rev. B*, 2013, **87**, (14), p. 140302
[23] Hua Y.-C., Cao B.-Y.: 'Ballistic-diffusive heat conduction in multiply-constrained nanostructures', *Int. J. Thermal Sci.*, 2016, **101**, pp. 126–132
[24] Zhou Y., Gong X., Xu B., *ET AL.*: 'First-principles and molecular dynamics study of thermoelectric transport properties of N-type silicon-based superlattice-nanocrystalline heterostructures', *J. Appl. Phys.*, 2017, **122**, (8), p. 085105
[25] Mohamadi M., Raisi A., Mehrabian M.A.: 'Numerical study of thermal conductivity reduction in nanolayered Si-Ge structures by solving the equation of phonon radiative transfer', *J. Serb. Soc. Comput. Mechan. (JSSCM)*, 2017, **11**, (1), pp. 29–45
[26] Jeng M.-S., Yang R., Song D., *ET AL.*: 'Modeling the thermal conductivity and phonon transport in nanoparticle composites using Monte Carlo simulation', *J. Heat Transfer*, 2008, **130**, (4), p. 042410